

# UCSF

## UC San Francisco Previously Published Works

### Title

Pharmacologic heat shock protein 70 induction confers cytoprotection against inflammation in gliovascular cells

### Permalink

<https://escholarship.org/uc/item/89d223fk>

### Journal

Glia, 63(7)

### ISSN

0894-1491

### Authors

Kacimi, Rachid  
Yenari, Midori A

### Publication Date

2015-07-01

### DOI

10.1002/glia.22811

Peer reviewed

# Pharmacologic Heat Shock Protein 70 Induction Confers Cytoprotection against Inflammation in Gliovascular Cells

Rachid Kacimi and Midori A. Yenari

The inhibition of the 90-kDa heat shock protein (HSP90) leads to upregulation of the 70-kDa-inducible HSP70. HSP70 has been previously shown to be neuroprotective and anti-inflammatory. Geldanamycin (GA) and other HSP90 inhibitors have emerged as promising therapeutic agents in cancer, presumably owing to their ability to upregulate HSP70. However, the effects of HSP90 inhibition in brain inflammation are still unclear. We investigate the effect of a panel of HSP90 inhibitors on endotoxin-activated microglia and eventual protection from brain-derived endothelial cells. Prior studies have shown that GA protects brain cells from oxidative stress. We show here that when astrocytes or microglial BV2 cells were pretreated with GA or other HSP90 inhibitors, endotoxin-induced cell death was reduced in cocultures of BV2 microglia and brain-derived endothelial cells (bEND.3). Endotoxin-stimulated BV2 cells led to increased nitric oxide (NO) and inducible nitric oxide synthase which was prevented by treatment with all HSP90 inhibitors. HSP90 inhibitors also prevented lipopolysaccharide (LPS)-induced BV2 cell death. We also found that HSP90 inhibition blocked nuclear translocation of nuclear factor kappa B and attenuated I $\kappa$ B $\alpha$  degradation, and inhibited LPS-activated JAK-STAT phosphorylation. We show that pharmacologic inhibition of HSP90 with subsequent HSP70 induction protects cells that comprise the cerebral vasculature against cell death owing to proinflammatory stimuli. This approach may have therapeutic potential in neurological conditions with an inflammatory component.

GLIA 2015;63:1200–1212

**Key words:** cytoprotection, HSP70, HSP90, microglia, endothelial cells

## Introduction

We and others have previously shown that the 70-kDa heat shock protein (HSP70) protects brain cells against ischemia and other insults (Stetler et al., 2010). One mechanism of this protective effect may be through its ability to prevent detrimental proinflammatory responses (Yenari et al., 2005). We previously showed that overexpression of HSP70 in transgenic animals protected against traumatic brain injury by decreasing blood–brain barrier (BBB) disruption and hemorrhage. This effect was correlated to the suppression of matrix metalloproteinases (Kim et al., 2013). Translating the beneficial effect of HSP70 to the clinical level may include the use of pharmacological inducers of HSP70, such as those compounds which inhibit the 90-kDa HSP90 (Kim et al., 2012).

HSP90 is another molecular chaperone in the same family as HSP70, and it is known to regulate HSP70 induction. It is normally bound to heat shock factor (HSF), but under the

conditions of stress, HSP90 dissociates from HSF, and HSF can bind the promoter of HSP70, heat shock element (Sharp et al., 1999). Thus, by inhibiting HSP90, HSP70 can be pharmacologically induced. Several HSP90 inhibitors (also referred to as HSP70 inducers) have already been studied as a potential cancer treatment, both at the preclinical and at the clinical levels (Hwang et al., 2009; Soga et al., 2013). Geldanamycin (GA) and its analog 17-allylamino-17-demethoxygeldanamycin (17-AAG), represent a class of HSP90 inhibiting drugs, the benzoquinone ansamycin antibiotics, capable of inducing HSP70 through its ability to bind and disrupt the function of HSP90 (Georgakis and Younes, 2005; Hwang et al., 2009; Kim et al., 2012; Miyata, 2005). HSP90 inhibitors, by virtue of their ability to induce HSP70, have been shown to promote the protection against tissue injury (Harrison et al., 2008; Kwon et al., 2008; Lu et al., 2002; Ouyang et al., 2005; Sonoda et al., 2010; Xu et al., 2003).

View this article online at [wileyonlinelibrary.com](http://wileyonlinelibrary.com). DOI: 10.1002/glia.22811

Published online March 20, 2015 in Wiley Online Library ([wileyonlinelibrary.com](http://wileyonlinelibrary.com)). Received June 10, 2014, Accepted for publication Feb 17, 2015.

Address correspondence to Midori A. Yenari, Department of Neurology, University of California, San Francisco Neurology (127) VAMC 4150 Clement St, San Francisco, California. E-mail: [yenari@alum.mit.edu](mailto:yenari@alum.mit.edu)

From the Department of Neurology, University of California, San Francisco & San Francisco Veterans Affairs Medical Center, San Francisco

Recent findings also highlight the role of HSPs in modulating immune response and the inflammatory pathways, and the benefit of overexpression of HSP70 and anti-HSP90 therapy against inflammation during infection, immune disease, or ischemia/reperfusion-induced injury such as experimental stroke (Jones et al., 2011; Kim et al., 2012; Poulaki et al., 2007; Rice et al., 2008; Tsan and Gao, 2009; Yenari et al., 2005; Zheng et al., 2008). To our knowledge, there have been no previous studies examining the role of HSP90 inhibitors in brain inflammation.

We previously developed a model of inflammation-induced brain endothelial cell injury in which we can study the effects of inflammatory responses on the cerebral vasculature (Kacimi et al., 2011). In this model, the application of the endotoxin lipopolysaccharide (LPS) to cocultures of brain-derived endothelial cells and microglia lead to endothelial cell death. We use this model to examine a panel of HSP90 inhibitors, and examine their potential in protecting cells of the brain's vasculature.

## Materials and Methods

### Materials

All reagents were of high grade and were purchased from Sigma with the following exceptions. RPMI, Dulbecco's modified Eagle's medium (DMEM), Calcein, and other culture reagents were purchased from Invitrogen (Grand Island, NY) and the UCSF cell-culture facility (UCSF, San Francisco, CA). Fetal bovine serum (FBS) defined was purchased from Hyclone Laboratories (Logan, UT). Selective HSP90 inhibitors: GA, 17-AAG, radicicol, and BIIB021 were purchased from Calbiochem (San Diego, CA). LPS (*Escherichia coli*, O26:B6) was purchased from Sigma (St. Louis, MO). The drugs were dissolved in DMSO or ethanol and stored at  $-20^{\circ}\text{C}$  and either used as final concentration of vehicle (0.1% v/v) or dried down and resuspended in phosphate-buffered saline (PBS)/0.1% bovine serum albumin (BSA). HSP antibodies were purchased from Assay design (Enzo Life sciences), for MAP stress-activated kinase anti-phospho-JNK/SAPK mAb (#4668) were from Cell Signaling Technology (Danvers, MA); anti-NF-kBp65 (# SC-8008), anti-I $\kappa$ B $\alpha$  (# SC-1643) and respective horseradish peroxidase-coupled secondary antibodies were purchased from Santa Cruz (Santa Cruz, CA) and antibodies against mouse HSP70i (#SPA-810) from Enzo Life Sciences, inducible nitric oxide synthase (iNOS) (# 61043), were from BD Biosciences (Lexington, KY); cyclooxygenase-2 (COX-2) antibody is from Cayman Chemical (Ann Arbor, MI [# 160106]).

### Cell Culture

**Glial Cell Preparation.** Primary mouse astrocytes were isolated and prepared by proteolytic dissociation of neonatal cortical tissue and cultured using standard protocols as described previously (Yenari et al., 2006). Brains obtained from 1- to 3-day-old pups were minced and resuspended in perfusion buffer with 10% of FBS. To

remove debris, the suspension then was passed through a filter (Falcon). Cells that passed through the filter were pelleted by centrifugation at 500g for 5 min, and the supernatant was removed. The pellet was washed twice, and resuspended in Minimal Essential Medium (MEM) containing 10% of FBS supplemented with antibiotics (penicillin/streptomycin, 100 U/mL). After 1 h of attachment to tissue culture plates, cells that were weakly attached or unattached (neuronal cells, endothelial cells, smooth muscle cells, and red blood cells) were rinsed free and discarded. Adherent cells either pure astrocytes or microglia-enriched mixed glial cells were grown and used for 1–3 passages as described previously (Yenari et al., 2006). Some astrocyte cultures were exposed to 5-h hypoxia followed by reoxygenation for 24 h, using an anoxia chamber as described previously (Lee et al., 2004). In astrocytes, hypoxia, unlike oxygen–glucose deprivation, does not cause significant cell stress or death. As a positive control, other astrocyte cultures were exposed to heat stress using a paradigm previously shown to induce endogenous HSP70 (Kim et al., 2002).

**BV2 Cells.** The immortalized mouse microglia cell line, BV2 cells, exhibits both the phenotypic and the functional properties of reactive microglia cells and is a suitable model of inflammation as described previously (Kacimi et al., 2011; Webster et al., 2013). Briefly, cells were grown and maintained in RPMI supplemented with 10% of FBS and antibiotics (penicillin/streptomycin, 100 U/mL). Under a humidified 5% CO<sub>2</sub>/95% air atmosphere and at 37 °C, cells were plated in 75-cm<sup>2</sup> cell-culture flask (Corning, Acton, MA) and were split twice a week. For the experiments, cells were placed on six-well dishes as described previously (Kacimi et al., 2011).

**BEND.3 Cells.** The immortalized mouse brain microvascular endothelial cell line, bEND.3, was purchased from American Type Culture Collection (Manassas, VA). Cells were grown in DMEM supplemented with 450 mg/dL of glucose, 10% of FBS defined, and antibiotics. For coculture of BV2 cells and microvascular endothelial cells, bEND.3 cells were grown to confluence in DMEM with serum, thereafter BV2 cells were seeded on the top of the monolayer and set to adhere for 24 h before each experimental design as described previously (Kacimi et al., 2011).

### Experimental Protocols

**Cell Treatment.** Cells were cultured to approximately 80% of confluence, and the cultures with a density of approximately  $0.5 \times 10^6$  cells were used. Similar culture densities were verified prior to use. Fresh serum-free media were added for 4–24 h before LPS or inhibitor treatments. All inhibitors were applied 1 h before experimental treatment and given in doses as follows unless otherwise specified: GA (100 nM), 17-AAG (500 nM), BIIB021 (100 nM), and radicicol (10  $\mu\text{M}$ ). LPS was used in a concentration of 1  $\mu\text{g}/\text{mL}$ , H<sub>2</sub>O<sub>2</sub> (500  $\mu\text{M}$ ), and Poly (I:C) 100  $\mu\text{g}/\text{mL}$ . These concentrations were based on our prior study in this model of endothelial cells and microglia, as well as preliminary dose–response assays for all the treatments used. The LPS, Poly (I:C), and H<sub>2</sub>O<sub>2</sub> concentrations were based on those used in the literature as well as that found in

our hands to cause approximately 60–70% of cell death. For the HSP90 inhibitors, we used optimal concentrations that inhibited NO and NO signaling proteins without observable cytotoxic effect on cells as described previously (Kacimi et al., 2011).

### Cell Transfection and HSP70 Knockdown

Standard siRNA transfection was used for transient silencing of Hsp72 in BV2 cells. Cells were incubated in six-well plates for 48–72 h with either nontargeting siRNA control or HSP70 smart pool siRNA constructs from Dharmacon/Thermo Scientific (Waltham, MA) in Opti-DMEM media. Lipofectamine RNAiMAX transfection reagent (Invitrogen) was used to enhance siRNA delivery according to the manufacturer's instructions. To validate our transfection assay, we used Alexa Fluor<sup>®</sup> Red Fluorescent Control siRNA as a positive control. Overall efficiency of transfection using this protocol was about 60–70% with minimal toxicity to the cells. After 2 days of transfection with either control siRNA or HSP70 siRNA for knockdown, cell-culture media were changed to serum-free defined media, cells were thereafter pretreated with 17-AAG for 1 h and subsequently incubated with the TLR4 agonist LPS or the TLR3 agonist Poly (I:C). In total, 24 h later, NO accumulation was evaluated using the Griess reagent as described in the methods below.

**Fluorescence Microscopy.** Fluorescence immunocytochemistry was performed on cells as described previously (Kacimi et al. 2011). The wells were washed twice in PBS and then fixed with acetone/methanol (1:1) for 5 min at  $-20^{\circ}\text{C}$ . Alternatively, cells were fixed in 4% of paraformaldehyde for 30 min at room temperature. The cells were then washed twice with PBS containing 0.2% of Triton X-100 for 15 min. Nonspecific binding sites were blocked in blocking buffer (2% BSA and 0.2% Triton X-100 in PBS) for 2 h. The cells were incubated with primary antibody-specific marker for the vascular unit cells as indicated at 1:100 dilution in blocking buffer overnight at  $4^{\circ}\text{C}$  and then washed three times with blocking buffer, 10 min per wash. The cells were incubated with either alexa or FITC-conjugated secondary antibody (Jackson ImmunoResearch, West Grove, PA) at 1:100 dilution in blocking buffer at room temperature for 1 h, then washed two times in blocking buffer, and one time in PBS, 10 min per wash. Fluorescence was visualized with an epifluorescence microscope (Zeiss Axiovert; Carl Zeiss), and the images were obtained on a PC computer using Axiomatic software (Zeiss).

**NO Measurement.** The accumulation of NO in cultures media was determined by the Greiss reagent using nitrite as standard as described previously (Han et al., 2002; Kacimi et al. 2011). After 24 h of incubation, serum-free media were removed and fresh media were added. LPS or vehicle was then added, and cells were returned to the incubator. After incubation for 24 or 48 h, aliquots of the incubation media were removed and either stored at  $-80^{\circ}\text{C}$  or used immediately for nitrite content analysis.

**Immunoblotting.** After each treatment period, cells plated on six-well or 60-mm dishes were washed with cold PBS, and scraped into 500- $\mu\text{L}$  lysis buffer. Lysates were sonicated and centrifuged for 5 min. The supernatant was collected and either used immediately or

frozen at  $-80^{\circ}\text{C}$ . Protein concentration was determined using the BCA protein assay (Pierce, Rockford, IL), and equal amounts of protein were loaded per lane onto 10–12% sodium dodecylsulfate–polyacrylamide gels, and were electrophoresed (SDS–PAGE) as described previously (Kacimi and Gerdes 2003; Kacimi et al. 2000, 2011). Gels were then transferred onto enhanced chemiluminescence (ECL)–nylon membranes in transfer buffer containing 48 mM of Tris, 150 mM of glycine, and 10% of methanol using a Transblot apparatus (Biorad, Hercules, CA) at 100 V for 1 h at  $4^{\circ}\text{C}$ . The membranes were saturated in PBS 0.1% Tween-20, and 5% nonfat dry milk for 1 h at room temperature and then probed with specific polyclonal antisera for iNOS and COX-2 in the same buffer for 1 h at room temperature with gentle agitation. Anti-phospho-JNK and phospho-JAK2 mAbs were from Cell Signaling Technology (Danvers, MA). For all antibodies used, working dilution was 1:500 and 1:1,000 for rabbit and mouse primary antibodies, respectively. The membranes were washed three times with PBS 0.1% Tween-20. Bound antibodies were identified after incubation with peroxidase-conjugated anti-rabbit antibodies (1:2,000 dilution in saturation buffer) for 1 h at room temperature. The membranes were then rewashed three times and the position of the individual proteins was detected by chemiluminescence ECL according to the manufacturer's instruction.

**Assessment of I $\kappa$ B $\alpha$  Degradation and Nuclear Factor Kappa B Nuclear Translocation.** I $\kappa$ B $\alpha$  in cytoplasmic extracts was detected by Western blot and nuclear translocation of the p65 nuclear factor kappa B (NF- $\kappa$ B) subunit was determined by immunofluorescence using specific antibodies against I $\kappa$ B $\alpha$  and NF- $\kappa$ B p65, respectively.

**Cell Viability Assays.** Cell viability was assessed by a diazo dye (Sun et al., 2006) 3-(4,5-dimethylthiazol-2-yl)-2,5-diphenyltetrazolium bromide (MTT) assay, that measures mitochondrial respiration, an index of cell viability. At the end of the observation period, media were harvested, and MTT was added. Afterward, the absorbance of each sample was read by a multiwell spectrophotometer at 570 nm of wavelength. Cell viability was calculated as the percentage of absorbance in each sample versus the control. Alternatively, *trypan* blue exclusion and calcein stain was assayed for cell viability (calcein stain) as described previously (Kacimi et al., 2000, 2011).

**Statistical Analysis.** All data were analyzed in a blinded fashion by the investigators unaware of the experimental condition. Significant differences were determined by either Student's two-tailed *t*-test for the comparison of the means of two samples or analysis of variance (ANOVA) for the comparison of more than two sample means followed by Newman–Keuls *post hoc* testing for multiple comparisons among sample means. The significance level was set at  $P < 0.05$ . Data are shown as mean  $\pm$  SEM.

## Results

We first established that heat shock and GA treatments led to HSP70 induction (Fig. 1A,B). GA dose dependently increased HSP70 in primary astrocyte cultures (Fig. 1B). Similarly, other HSP90 inhibitors 17-AAG, radicicol, and BIIB021 also

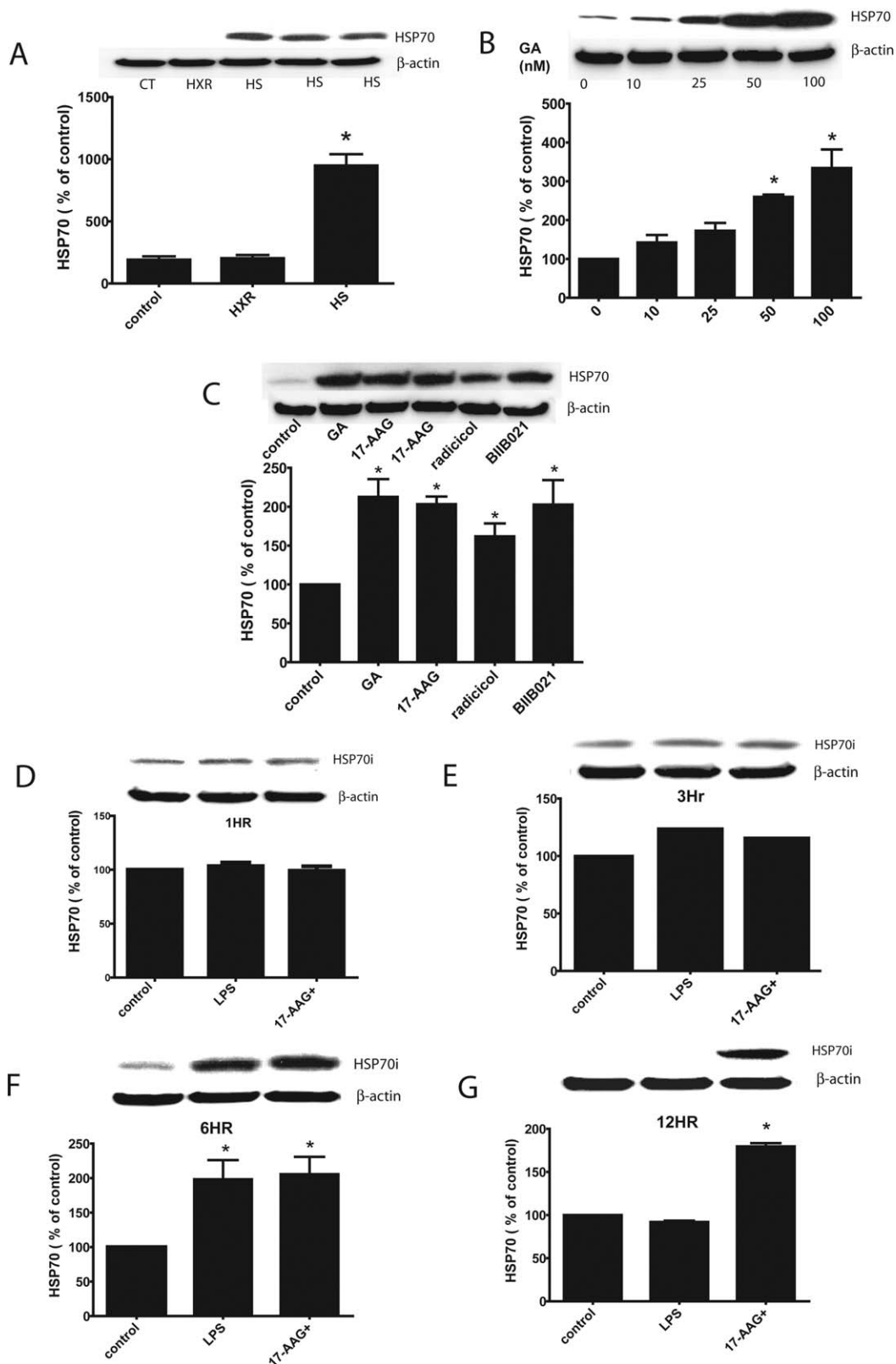


**FIGURE 1:** A: Heat shock induces HSP70 in astrocytes. The schematic representation of Western blot of primary astrocyte whole-cell extracts using a mouse antibody specific for inducible HSP70 and graph to quantify these observations. HXR: 5 h hypoxia/24 h reoxygenation, HS: heat shock; 30 min at 42.5 °C + 1-day recovery, CT: control cultures were not exposed to insults. B: GA mimics the heat shock response by inducing HSP70 in astrocytes. A representative Western blot and graph of the data are shown. The treatment of astrocytes with GA for 24 h leads to dose-dependent increases of HSP70 protein, much like that seen with heat shock treatment. C: GA and similar HSP90 inhibitors increased HSP70 in astrocytes. The treatment of astrocytes with GA and GA analog 17-AAG, radicicol, or BIIB021 for 24 h induces HSP70 protein expression to similar levels as GA and heat shock treatment. D–G: Kinetics of HSP70 induction in the setting of endotoxin treatment with and without HSP90 inhibition by 17-AAG. BV2 cells were treated with LPS and the time course of HSP70 induction was determined at different times (1–12 h) with and without treatment with 17-AAG. Optical densitometric values were normalized to  $\beta$ -actin as a housekeeping control, and are expressed as the percentage of controls. Data are shown as mean  $\pm$  SEM,  $n = 3$ –5 independent experiments \* $P < 0.05$ .

induced HSP70 (Fig. 1C). We then determined the kinetics of HSP70 induction in the setting of endotoxin treatment with and without HSP90 inhibition by 17-AAG (Fig. 1D). BV2 cells were treated with LPS and the time course of HSP70 induction was determined at different times with and without treatment with 17-AAG. We found that LPS itself induced HSP70 as early as 1-h postapplication, then continued to increase 3 and 6 h later, but was no longer detectable by 12 h. In the presence of 17-AAG, induction of HSP70 above that by LPS alone was evident by 6 h and persisted at 12 h when LPS-induced HSP70 was no longer present.

We then treated astrocytes exposed to H<sub>2</sub>O<sub>2</sub> with these compounds 24 h prior to injury, and found that in all cases, they protected against oxidative stress (Fig. 2). The concentration chosen was based on the pilot studies to determine the highest concentration of each compound that did not lead to toxicity (as evidenced by morphological changes in uninjured astrocytes or b.End.3 cells, data not shown). These agents also protected microglial BV2 cells from H<sub>2</sub>O<sub>2</sub>-induced injury (data not shown).

We then explored the effect of HSP70 induction and potential anti-inflammatory effects. Primary microglia-enriched astrocyte cultures (mixed glial cultures prepared without the removal of the microglia) were exposed to LPS, leading to the activation of primarily microglia, but astrocytes as well, and leading to increased nitric oxide (NO) generation. The application of HSP90 inhibitors in concentrations previously shown to be cytoprotective, all led to the abrogation of NO production (Fig. 2D).

We next turned to a coculture model of brain-derived endothelial cells and microglia, where LPS treatment leads to endothelial cell death via microglial activation (Kacimi et al., 2011). Cocultures of bEnd.3 and BV2 cells were prepared, and then treated with HSP90 inhibitors followed by LPS exposure. In all cases, HSP90 inhibitors led to improved cell viability (Fig. 3). As LPS treatment in this model leads predominantly to bEnd.3 cell death, the protection was largely owing to the protection of bEnd.3 cells. However, when cultured alone, BV2 cells are also vulnerable to LPS exposure, and this vulnerability can be prevented by treatment with HSP90 inhibitors. BV2 cell death was reduced as assayed by calcein uptake and MTT (Fig. 4). To determine whether these HSP70 inducers might exhibit anti-inflammatory effects, we measured both iNOS protein levels and NO accumulation by BV2 cells after LPS exposure. In all cases, HSP90 inhibitor treatment led to the suppression of NO production and iNOS protein expression (Fig. 5A,B). Prior study has shown that HSP70's immune modulating properties are owing to the interactions with TLR4, the receptor upon which LPS acts. However, other study, including that from our own lab, has shown that HSP70 can also interfere with

the proinflammatory transcription factor NF- $\kappa$ B) (Ran et al., 2004; Zheng et al., 2008). To determine whether the anti-inflammatory mechanism is through an interaction through TLR4 in our model or an alternate mechanism, we treated BV2 cells with the TLR3 agonist Poly (I:C). Poly (I:C) treatment also led to NO accumulation; however, treatment with the same HSP90 inhibitors also suppressed NO generation by Poly (I:C) in a manner similar to LPS, suggesting that the anti-inflammatory effect of HSP70 is not specific to TLR4 signaling (Fig. 5C).

To determine whether the anti-inflammatory effect of HSP70 induction was through NF- $\kappa$ B or other factors, we assayed for NF- $\kappa$ B nuclear translocation, I $\kappa$ B $\alpha$  degradation, and JAK-STAT and JNK activation. We chose these factors based on our previous study that showed that these are the main transcription factors that lead to iNOS induction by LPS in BV2 cells (Kacimi et al., 2011). Accordingly, we found that the HSP90 inhibitors prevented nuclear NF- $\kappa$ B translocation, I $\kappa$ B $\alpha$  degradation, and JAK2 phosphorylation after LPS exposure (Fig. 6). JNK phosphorylation was affected to lesser extent.

To establish whether the anti-inflammatory effect of 17-AAG was owing to the induction of HSP70, we used siRNA to knock down HSP70 in BV2 cells. Using control siRNA containing Alexa Fluor to identify cells which took up the siRNA, we found that approximately 60% of the cells took up the reagent without any significant cytotoxicity (Fig. 7A). In addition, to estimate the extent of HSP70 knockdown, we performed Western blots of HSP70. Our data show that 17-AAG increased HSP70, but this was prevented by HSP70 siRNA knockdown (Fig. 7B). The knockdown of HSP70 blunted the anti-inflammatory effect of 17-AAG against TLR3 and TLR4 agonists as estimated by nitrite (NO) accumulation in the culture media (Fig. 7C,D). The proportion of blunting was roughly similar to the extent of HSP70 knockdown. These data together indicate that HSP70 is responsible for the anti-inflammatory effect of 17-AAG. A proposed mechanism of 17-AAG's anti-inflammatory response against TLR4 and TLR3 in microglia BV2 cells is shown in Fig. 8.

## Discussion

We show that HSP70 can be pharmacologically induced by a panel of HSP90 inhibitors, and that this induction can protect brain-derived endothelial cells and astrocytes against oxidative and inflammatory stress. Pharmacologic HSP70 induction in microglial cells also exhibited anti-inflammatory responses. Further, we show that this is largely through the induction of HSP70 as knockdown of HSP70 led to the reduction of this anti-inflammatory effect. These observations are in line with that previously shown by us, where we used

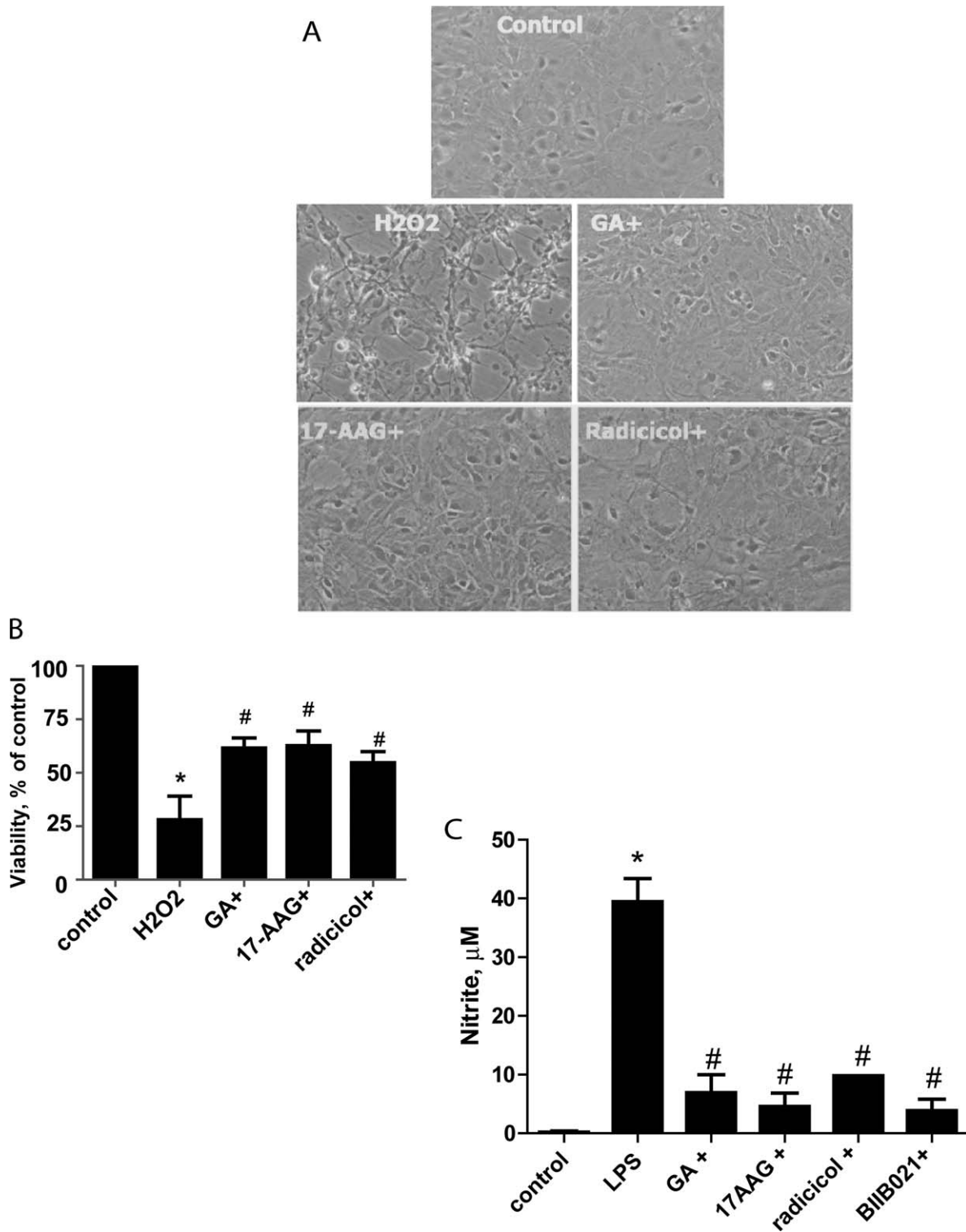


**FIGURE 2: HSP90 inhibitors protect astrocytes against oxidative stress.** **A:** Astrocytes were treated with GA+, 17-AAG (17-AAG+), radicicol (Radicol+), or vehicle (H<sub>2</sub>O<sub>2</sub>) 24 h prior to H<sub>2</sub>O<sub>2</sub> exposure. Light microscopy shows astrocyte damage owing to 2 h H<sub>2</sub>O<sub>2</sub> exposure, and this was prevented by all three HSP90 inhibitors. Control, uninjured, and untreated cultures are shown for comparison (Control). **B:** Cell viability was quantified by MTT. *n* = 3–5 experiments, *P* < 0.05 \*versus control, # versus H<sub>2</sub>O<sub>2</sub>. **C:** HSP90 inhibitors prevent LPS-induced NO generation in glial cells. Mouse primary glial-mixed cells (astrocytes plus ~10% microglia) were treated either alone with vehicle (control), LPS alone (LPS), or LPS plus individual HSP90 inhibitors (GA+, 17-AAG+, radicicol+, and BIIB021+) for 24 h, followed by media change, then LPS was added for another 24 h. Nitrite accumulation was measured by the Griess reagent. *n* = 5–8 experiments, \**P* < 0.05 versus control, # versus LPS alone.

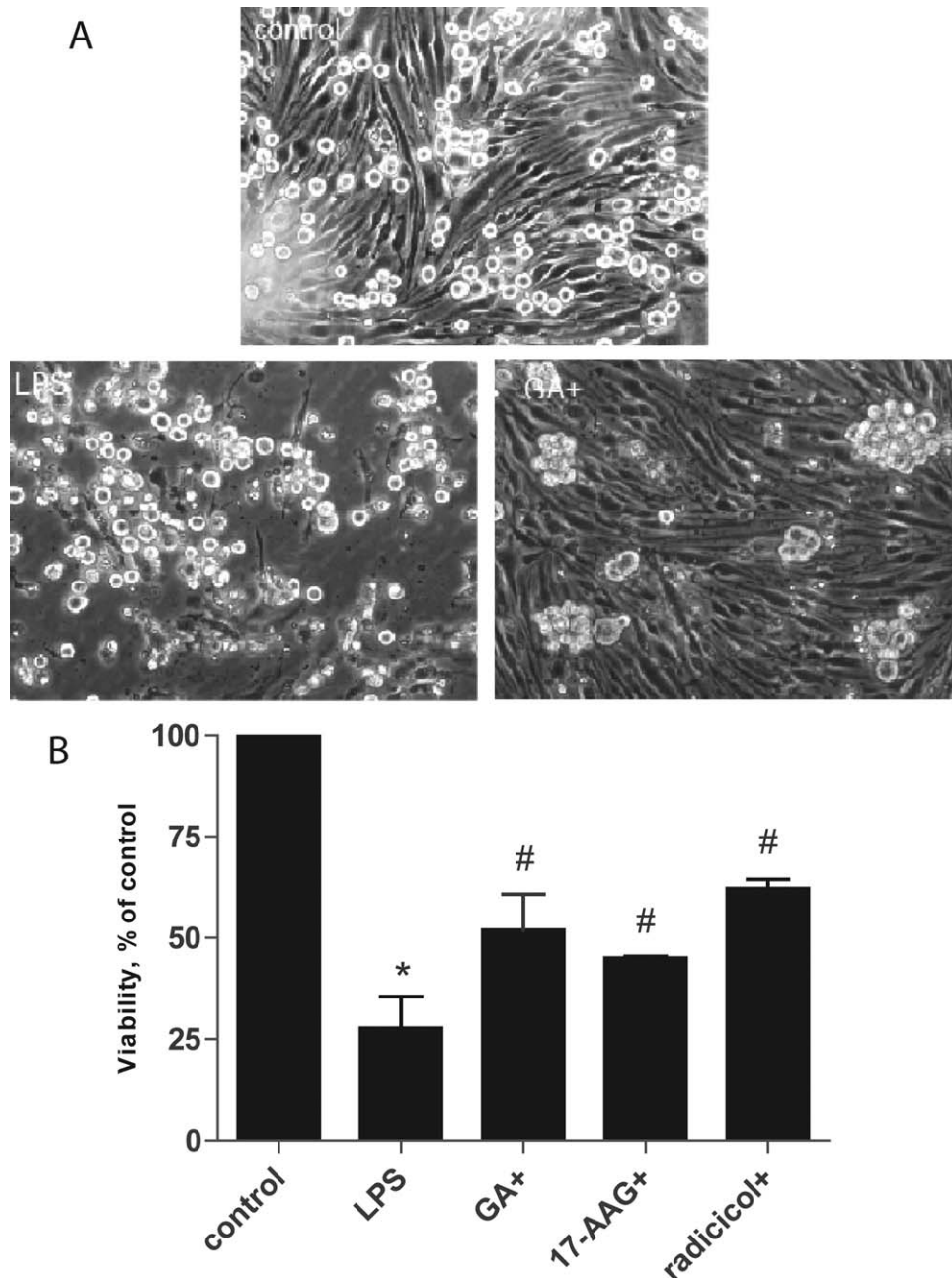


**FIGURE 3:** HSP90 inhibitors prevented endothelial cell death owing to microglial activation. **A:** Although LPS did not affect bEnd.3 cells alone (bEnd.3 + LPS), when cultured with BV2 cells (LPS), LPS increased cell death and monolayer disruption of predominantly bEnd.3 cells compared with control cocultures (control). The treatment of cocultures with LPS plus GA+ prevented monolayer disruption. **B:** Quantitation of coculture experiments show that cell viability is decreased after LPS treatment, and this is prevented by GA (GA+), 17-AAG (17-AAG+), radicicol (radicicol+). GA: geldanamycin (0.1–0.2 M), 17-AAG, and (0.5–1 mM); radicicol: (RDC, 10  $\mu$ M).  $n = 4$ –6 independent observations, \* $P < 0.05$  versus control, # $P < 0.05$  versus LPS.

genetic approaches to selectively overexpress HSP70 (Lee et al., 2005; Zheng et al., 2008). As it is not possible to genetically overexpress HSP70 in humans, we show a potentially translatable pharmacological means of doing so. These data suggest a therapeutic potential for HSP90 inhibitors to protect from proinflammatory insults, such as that seen in stroke, brain trauma, and neuroinflammation. We previously

showed that HSP70 overexpression in either transgenic mice or cells treated with a viral vector encoding HSP70 inhibits the generation and activation of proteases implicated in the destruction of the brain's extracellular matrix (Lee et al., 2004) and decreases BBB disruption and subsequent brain hemorrhage (Kim et al., 2002). Thus, pharmacological HSP70 induction has the potential to treat clinical conditions



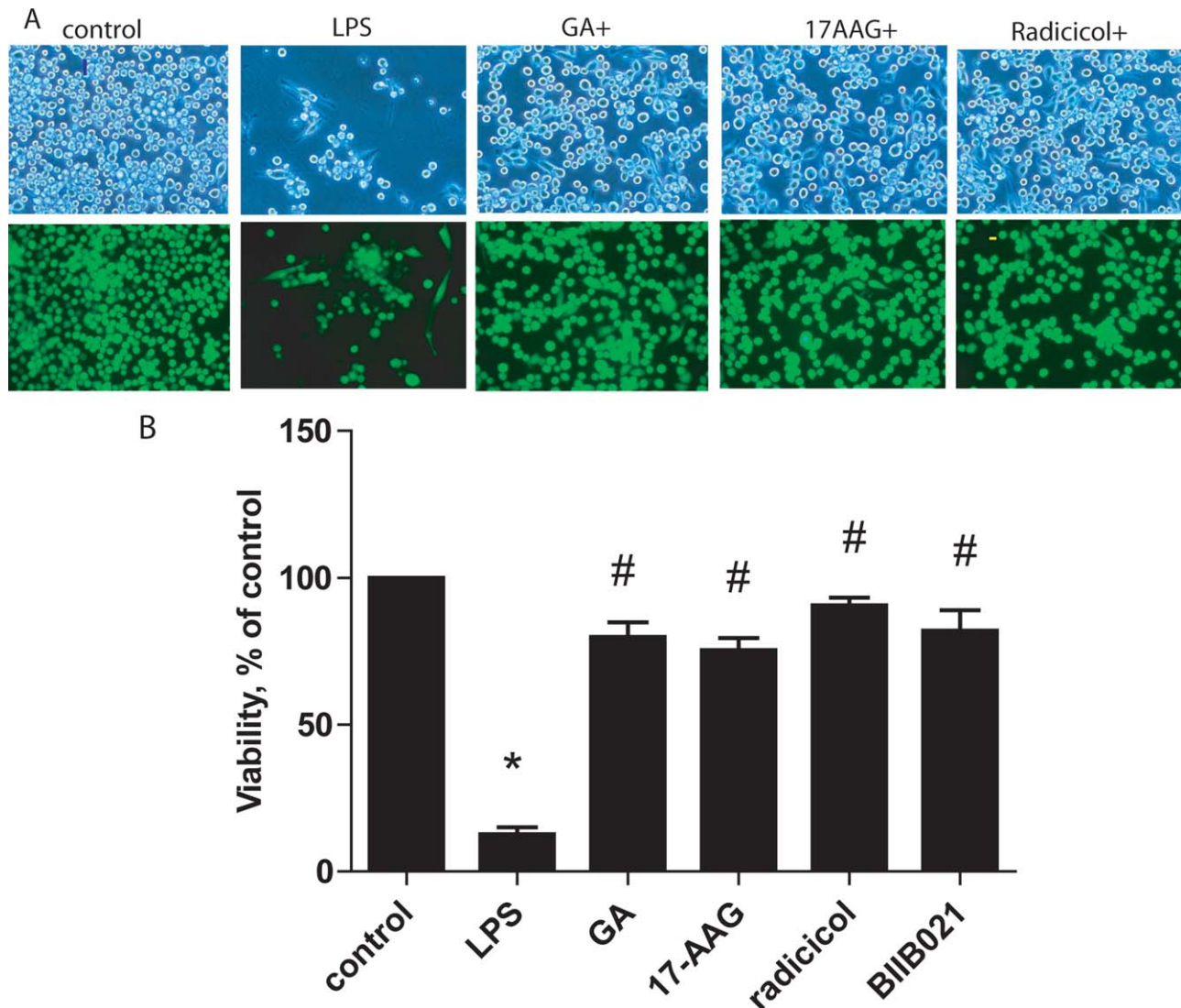


**FIGURE 4:** GA prevents LPS-induced injury in microglia BV2 cells. **A:** BV2 cells were treated with LPS or LPS plus HSP90 inhibitors for 24 h. Light microscopy (blue cells) or green live cell with calcein immunofluorescence shows LPS-induced BV2 cell injury, which was prevented by all three HSP90 inhibitors. **B:** MTT assay shows that four different HSP90 inhibitors prevented LPS induced death of BV2 cells.  $P < 0.05$  versus \*control, # versus LPS. [Color figure can be viewed in the online issue, which is available at [wileyonlinelibrary.com](http://wileyonlinelibrary.com).]

where the preservation of the BBB and prevention of brain hemorrhage may be desirable.

We studied a panel of HSP90 inhibitors that have been previously studied at the clinical level in patients with cancer (Jhaveri et al., 2012). We replicated prior studies of GA which showed protection in brain cells (Xu et al., 2003), then explored whether similar protection could be observed with other inhibitors. Although GA has been previously shown to protect against experimental stroke (Kwon et al., 2008; Lu et al., 2002) and related brain injury models (Ouyang et al., 2005; Xiao et al., 1999), it was poorly tolerated in humans owing to liver toxicity (Supko et al., 1995). Thus, we expanded our observations to include additional HSP90 inhibitors, radicicol, 17-AAG, and BIIB021. 17-AAG was developed as a less

toxic analogue of GA, and is the most widely studied HSP90 inhibitor in more than 30 clinical studies including some at the Phase 3 level (Porter et al., 2010). BIIB021 has also been studied in humans in Phase 2 studies of cancer, and it is also available in a form that can be given orally (Lundgren et al., 2009; Porter et al., 2010). Radicicol was identified as a naturally occurring HSP90 inhibitor, but was unfortunately found to degrade quickly *in vivo* (Porter et al., 2010). Most of these studies were carried out in cancer trials, but little work has been carried out in cell injury models although radicicol was shown to protect renal cells from ischemia-like insults (Sonoda et al., 2010). Regardless, we found similar effects for all HSP90 inhibitors in our *in vitro* model, and would support further investigation of any or all of these compounds.

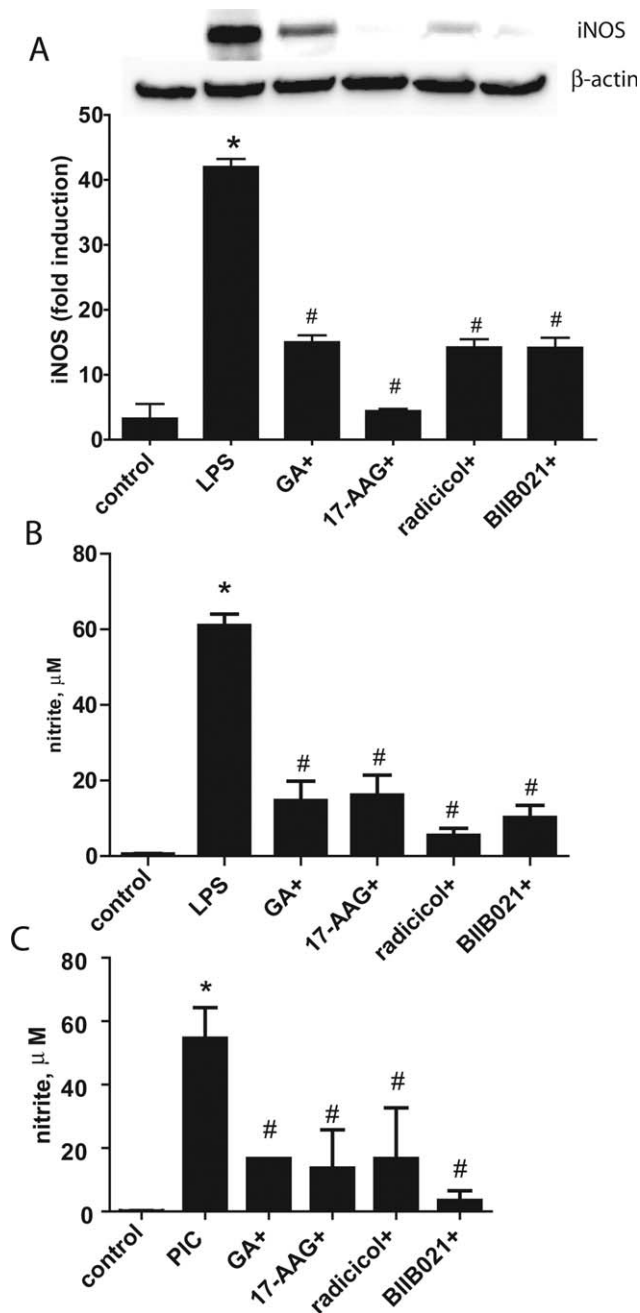


**FIGURE 5:** HSP90 inhibitors decrease iNOS induction and NO accumulation by LPS in microglia. BV2 cells were treated with LPS, vehicle, or LPS plus HSP90 inhibitors for 24 h. **A:** iNOS protein induction by LPS is prevented by all HSP90 inhibitors. **B:** Nitrite accumulation as measured by Griess reagent shows that LPS increases NO, whereas HSP90 inhibitors all decrease it.  $n = 5-8$  experiments,  $P < 0.05$  was considered significant. \*Versus control, # versus LPS. **C:** HSP90 inhibitors prevent TLR3 agonist induced NO in BV2 cells. BV2 microglia cells were treated with the TLR3 agonist, Poly (I:C) (PIC), either alone with vehicle or HSP90 inhibitors for 24 h. NO levels were estimated by the amount of nitrite accumulation using the Griess reagent.  $n = 5-8$  experiments,  $P < 0.05$ , \*versus control, # versus LPS.

We used an *in vitro* model of endotoxin-activated microglia which in turn led to damage to brain endothelial cells (Kacimi et al., 2011). This model could be said to model the aspects of brain ischemia/trauma, neuroinflammation, and sepsis where injurious or inflammatory stimuli activate immune cells and lead to BBB disruption (Alvarez et al., 1996; Hanisch, 2002; Lehnardt, 2010). BBB disruption can lead to secondary damage owing to the leakage of serum proteins into the brain leading to edema and cytotoxicity. With extreme BBB disruption, hemorrhage can occur. Thus, by protecting the brain's vasculature from immune attack through HSP70 induction, secondary consequences of brain injury could be ameliorated. This beneficial effect on endothelial cells was related to the suppression of immune responses in microglia.

The past studies have indicated that HSP70 can act as ligands for the Toll-like receptors (TLRs) present on immune cells including microglia (Giffard et al., 2008). In order for HSP70 to bind TLRs, it would need to be extracellular. In our model, HSP70 was generated intracellularly, and while it is possible that it could have been secreted, our data suggest that it likely acts in the intracellular compartment. Furthermore, HSP70 binding to TLRs tends to result in proinflammatory signaling, whereas our data indicate that its actions are anti-inflammatory.

LPS was used to stimulate NO production and iNOS protein synthesis in microglia, and these stimulated microglia led to endothelial cell disruption. The treatment with HSP90 inhibitors suppressed LPS-induced activation of microglia with parallel decreases in endothelial cell death. As LPS activates microglia by binding and activating the TLR4 pathway (Holm et al., 2012), we explored whether other TLR pathways might be similarly affected. Interestingly, GA also inhibited NO and iNOS generation by the TLR3 agonist Poly (I:C). Thus, the anti-inflammatory effect of HSP70 is likely downstream of the TLRs, and probably also acts intracellularly where it is generated through HSP90 inhibition.

Prior work relating to HSP70 and its ability to suppress immune responses has also indicated that HSP70 may interfere with the activation of proinflammatory transcription factors such as NF- $\kappa$ B (Ran et al., 2004; Zheng et al., 2008). We previously showed that in our model system, LPS-activated microglia lead to proinflammatory responses through NF- $\kappa$ B and JAK/STAT activation, and these responses could be inhibited by their respective inhibitors (Kacimi et al., 2011). Accordingly, we found that HSP90 inhibitors prevented I $\kappa$ B degradation, nuclear NF- $\kappa$ B translocation, and JAK-STAT phosphorylation owing to LPS. Thus, the mechanism of HSP90 inhibitors on inflammation may be related to the inhibition of the proinflammatory factors.

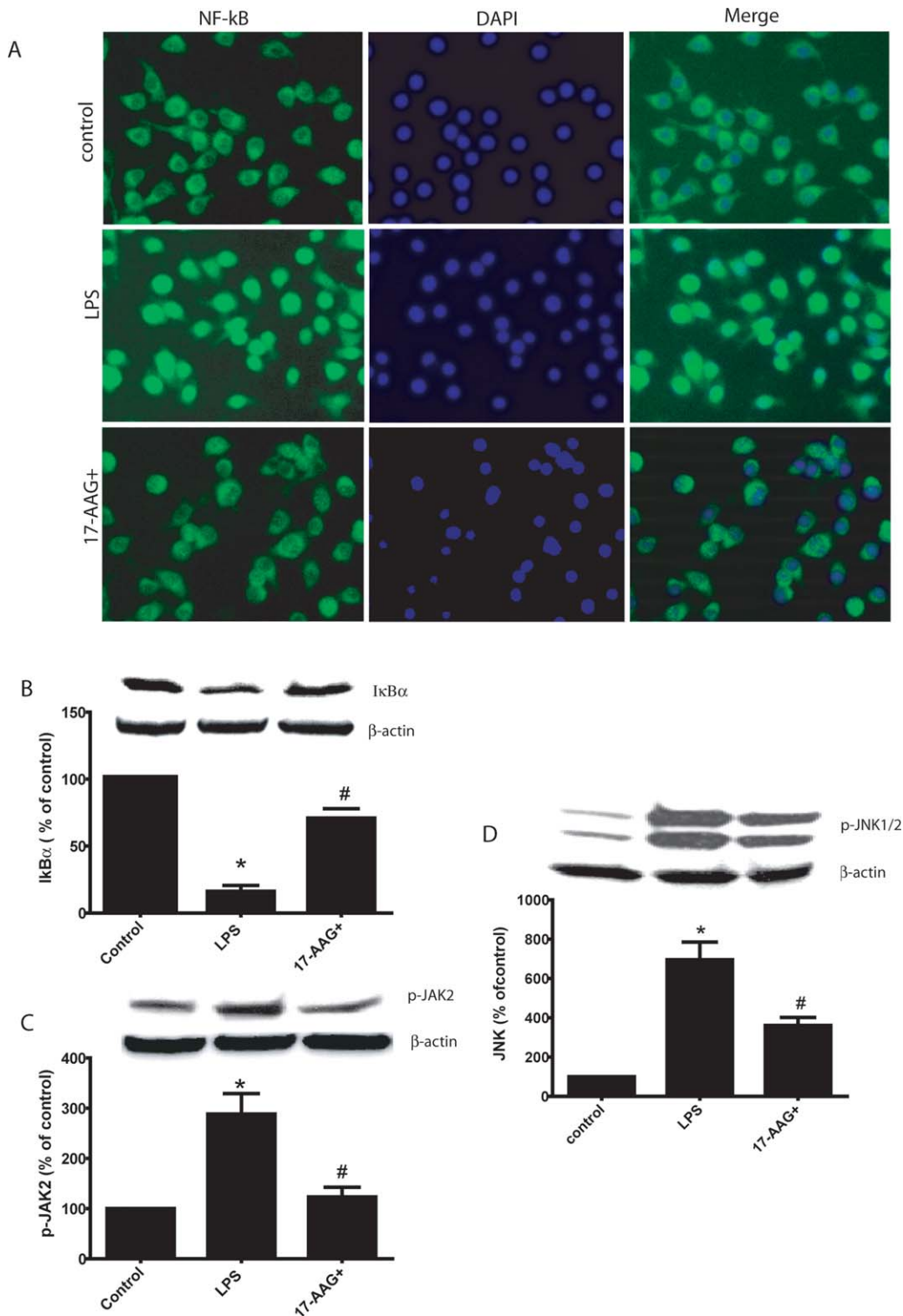


**FIGURE 6:** A: Immunofluorescent stains of NF-κB in BV2 cells show predominantly cytosolic staining in unstimulated control cells (control). LPS treatment led to overall NF-κB upregulation with staining within the nucleus (LPS). The treatment with 17-AAG (17-AAG+) prevented the LPS-induced NF-κB upregulation and nuclear staining is decreased. Cells were also stained with DAPI to delineate nuclei. Merging (Merge) of the two stains shows NF-κB relative to the nucleus. B: Western blots of BV2 cells show that LPS decreases the expression of NF-κB's endogenous inhibitor IκBα. This is consistent with NF-κB activation as IκB is degraded, and thus permitting NF-κB to translocate to the nucleus. This decrease is prevented by 17-AAG treatment. C and D: Similarly, LPS led to increases in phosphorylated JAK2 (p-JAK2) (C) and JNK1/2 (p-JNK1/2) (D). 17-AAG inhibited pJAK2 expression, and to a lesser extent, pJNK1/2. β-Actin is shown as a housekeeping control. Data in the graphs are expressed as the mean ± SEM of *n* = 5 independent experiments. *P* < 0.05 \*versus control, # versus LPS. [Color figure can be viewed in the online issue, which is available at [wileyonlinelibrary.com](http://wileyonlinelibrary.com).]

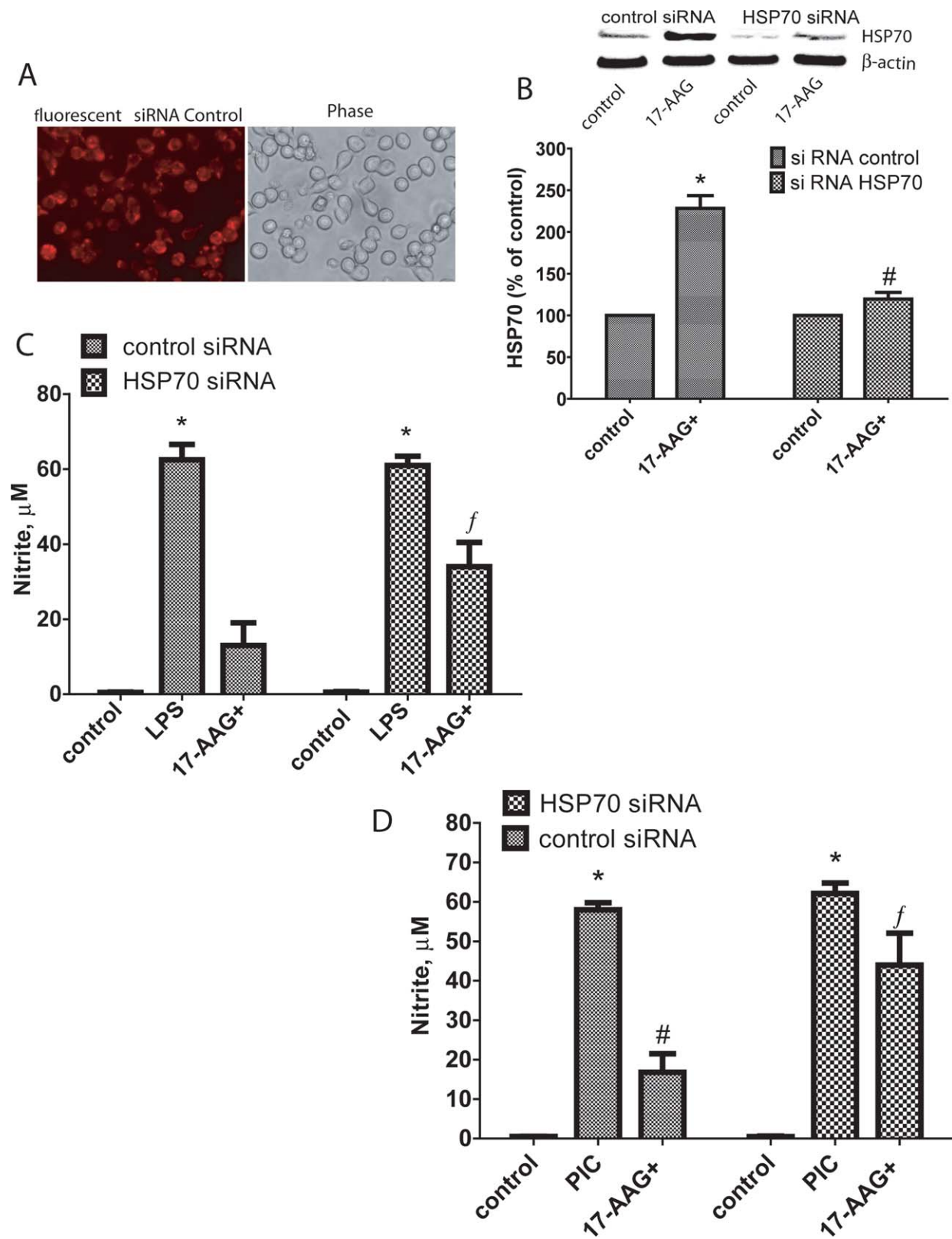


**FIGURE 7: HSP70 gene knockdown prevents 17-AAG anti-inflammatory response against TLR4 and TLR3 in microglia BV2.** **A:** BV2 cells were transfected with control siRNA linked to Alexa Fluor as a marker of cell uptake. Fluorescent imaging (fluorescent siRNA Control) shows cells which took up the siRNA as evidenced by the red stain. Phase contrast (Phase) delineates all of the cells from the same field, and these cells do not demonstrate any obvious cytotoxicity. **B:** BV2 cells were transfected with either control siRNA or siRNA against HSP70. Two days after transfection, culture media was changed to serum-free defined media, and cells were treated with 17-AAG or vehicle (control) for 24 h. Western blot was used to determine the efficacy of HSP70 silencing. Cultures in which HSP70 was knocked down failed to induce HSP70 by 17-AAG (B). Data in the graphs are expressed as the mean  $\pm$  SEM of  $n = 3$  independent experiments. \* $P < 0.05$  versus control, #versus 17-AAG treatment in cells in which HSP70 was knocked down. **C, D:** BV2 cells were transfected with either control siRNA or HSP70 siRNA for 48 h. Two days after transfection of the BV2 cells, culture media was changed to serum-free defined media, then treated with 17-AAG for 1 h, and incubated with the TLR4 agonist LPS (C) or the TLR3 agonist Poly (I:C [PIC]) (D). Control cultures (control) were treated with siRNA but not exposed to agonists. Twenty-four hours later, NO was estimated by measuring nitrite accumulation using the Griess reagent. Data in the graphs are expressed as the mean  $\pm$  SEM of  $n = 5$  independent experiments.  $P < 0.05$  \* versus control, # versus LPS or PIC treatment,  $f$  versus LPS or PIC treatment in cells in which HSP70 was knocked down. [Color figure can be viewed in the online issue, which is available at [wileyonlinelibrary.com](http://wileyonlinelibrary.com).]

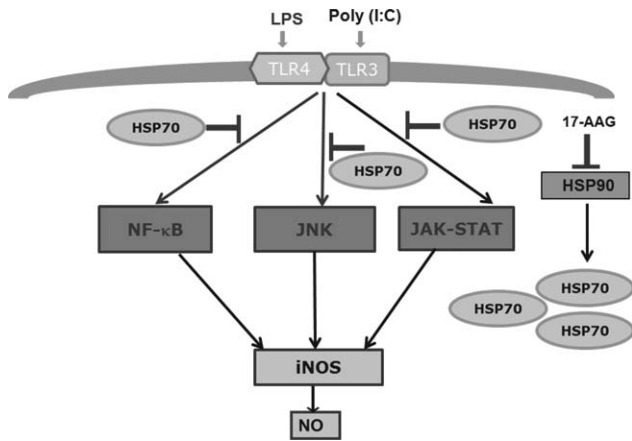


**FIGURE 8: Proposed mechanism of 17-AAG anti-inflammatory response against TLR4 and TLR3 in microglia BV2 cells.** LPS and Poly (I:C) binds to TLR4 and TLR3, respectively, on the surface of microglia, leading to the activation of several downstream signaling pathways: NF-κB, JAK-STAT, and JNK (JNK kinase) that lead to iNOS upregulation and the production of NO. The HSP90 inhibitor 17-AAG induced HSP70, which, in turn, suppressed the inflammatory response via blockade of NF-κB, JAK-STAT, and JNK signaling pathways responsible for iNOS induction and NO generation.

## Conclusions

In sum, HSP90 inhibitors induce HSP70, lead to anti-inflammatory effects, and protect brain-derived endothelial cells from death. These inhibitors should be studied in appropriate *in vivo* models of brain injury and inflammation. The work from our lab indicates that at least GA and 17-AAG will penetrate into the brain after parenteral administration, and will decrease BBB disruption and brain hemorrhage (Kim et al., 2015). Future work should be considered in terms of bringing one or more of these compounds to the clinic for neurological disorders.

## Acknowledgment

Grant sponsor: The National Institutes of Health; Grant number: NS40516; Grant sponsor: Veteran's Merit Award; Grant number: BX000589; Grant sponsor: The Department of Defense; Grant number: DAMD17-03-1-0532; Grant sponsor: The Northern California Institute for Research and Education, Resources of the Veterans Affairs Medical Center, San Francisco, California.

## References

Alvarez JI, Katayama T, Prat A. 2013. Glial influence on the blood brain barrier. *Glia* 61:1939–1958.

Georgakis GV, Younes A. 2005. Heat-shock protein 90 inhibitors in cancer therapy: 17AAG and beyond. *Future Oncol* 1:273–281.

Giffard RG, Han RQ, Emery JF, Duan M, Pittet JF. 2008. Regulation of apoptotic and inflammatory cell signaling in cerebral ischemia: The complex roles of heat shock protein 70. *Anesthesiology* 109:339–348.

## Kacimi and Yenari: HSP70 Induction Protects glio-Vascular Cells

Han HS, Qiao Y, Karabiyikoglu M, Giffard RG, Yenari MA. 2002. Influence of mild hypothermia on inducible nitric oxide synthase expression and reactive nitrogen production in experimental stroke and inflammation. *J Neurosci* 22:3921–3928.

Hanisch U-K. 2002. Microglia as a source and target of cytokines. *Glia* 40:140–155.

Harrison EM, Sharpe E, Bellamy CO, McNally SJ, Devey L, Garden OJ, Ross JA, Wigmore SJ. 2008. Heat shock protein 90-binding agents protect renal cells from oxidative stress and reduce kidney ischemia-reperfusion injury. *Am J Physiol Renal Physiol* 295:F397–F405.

Holm TH, Draeby D, Owens T. 2012. Microglia are required for astroglial toll-like receptor 4 response and for optimal TLR2 and TLR3 response. *Glia* 60: 630–638.

Hwang M, Moretti L, Lu B. 2009. HSP90 inhibitors: Multi-targeted antitumor effects and novel combinatorial therapeutic approaches in cancer therapy. *Curr Med Chem* 16:3081–3092.

Jhaveri K, Taldone T, Modi S, Chiosio G. 2012. Advances in the clinical development of heat shock protein 90 (Hsp90) inhibitors in cancers. *Biochim Biophys Acta* 1823:742–755.

Jones Q, Voegelé TS, Li G, Chen Y, Currie RW. 2011. Heat shock proteins protect against ischemia and inflammation through multiple mechanisms. *Inflamm Allergy Drug Targets* 10:247–259.

Kacimi R, Chentoufi J, Honbo N, Long CS, Karliner JS. 2000. Hypoxia differentially regulates stress proteins in cultured cardiomyocytes: Role of the p38 stress-activated kinase signaling cascade, and relation to cytoprotection. *Cardiovasc Res* 46:139–150.

Kacimi R, Gerdes AM. 2003. Alterations in G protein and MAP kinase signaling pathways during cardiac remodeling in hypertension and heart failure. *Hypertension* 41:968–977.

Kacimi R, Giffard RG, Yenari MA. 2011. Endotoxin-activated microglia injure brain derived endothelial cells via NF-kappaB, JAK-STAT and JNK stress kinase pathways. *J Inflamm* 8:7.

Kim JY, Kim YJ, Giffard RG, Yenari MA, Lee JE. 2002. Heat treatment and hsp70-overexpression suppressed matrix metalloproteinases in the primary astrocytes after ischemia-like injury. *Neurology* 58:A364.

Kim N, Kim JY, Yenari MA. 2012. Anti-inflammatory properties and pharmacological induction of Hsp70 after brain injury. *Inflammopharmacology* 20:177–185.

Kim N, Kim JY, Yenari MA. 2015. Pharmacological induction of the 70-kDa heat shock protein protects against brain injury. *Neuroscience* 284:912–919.

Kim JY, Kim N, Zheng Z, Lee JE, Yenari MA. 2013. The 70 kDa heat shock protein protects against experimental traumatic brain injury. *Neurobiol Dis* 58:289–295.

Kwon HM, Kim Y, Yang SI, Kim YJ, Lee SH, Yoon BW. 2008. Geldanamycin protects rat brain through overexpression of HSP70 and reducing brain edema after cerebral focal ischemia. *Neuro Res* 30:740–745.

Lee JE, Kim YJ, Kim JY, Lee WT, Yenari MA, Giffard RG. 2004. The 70 kDa heat shock protein suppresses matrix metalloproteinases in astrocytes. *Neuroreport* 15:499–502.

Lee JE, Yoon YJ, Moseley ME, Yenari MA. 2005. Reduction in levels of matrix metalloproteinases and increased expression of tissue inhibitor of metalloproteinase-2 in response to mild hypothermia therapy in experimental stroke. *J Neurosurg* 103:289–297.

Lehnardt S. 2010. Innate immunity and neuroinflammation in the CNS: The role of microglia in Toll-like receptor-mediated neuronal injury. *J Glia* 58: 253–263.

Lu A, Ran R, Parmentier-Batteur S, Nee A, Sharp FR. 2002. Geldanamycin induces heat shock proteins in brain and protects against focal cerebral ischemia. *J Neurochem* 81:355–364.

Lundgren K, Zhang H, Brekken J, Huser N, Powell RE, Timple N, Busch DJ, Neely L, Sensintaffar JL, Yang YC, McKenzie A, Friedman J, Scannevin R, Kamal A, Hong K, Kasibhatla SR, Boehm MF, Burrows FJ. 2009. BIB021, an orally available, fully synthetic small-molecule inhibitor of the heat shock protein Hsp90. *Mol Cancer Ther* 8:921–929.

- Miyata Y. 2005. Hsp90 inhibitor geldanamycin and its derivatives as novel cancer chemotherapeutic agents. *Curr Pharm Des* 11:1131–1138.
- Ouyang YB, Xu L, Giffard RG. 2005. Geldanamycin treatment reduces delayed CA1 damage in mouse hippocampal organotypic cultures subjected to oxygen glucose deprivation. *Neurosci Lett* 380:229–233.
- Porter JR, Fritz CC, Depew KM. 2010. Discovery and development of Hsp90 inhibitors: A promising pathway for cancer therapy. *Curr Opin Chem Biol* 14:412–420.
- Poulaki V, Iliaki E, Mitsiades N, Mitsiades CS, Paulus YN, Bula DV, Gragoudas ES, Miller JW. 2007. Inhibition of Hsp90 attenuates inflammation in endotoxin-induced uveitis. *FASEB J* 21:2113–2123.
- Ran R, Lu A, Zhang L, Tang Y, Zhu H, Xu H, Feng Y, Han C, Zhou G, Rigby AC, Sharp FR. 2004. Hsp70 promotes TNF-mediated apoptosis by binding IKK gamma and impairing NF-kappa B survival signaling. *Genes Dev* 18:1466–1481.
- Rice JW, Veal JM, Fadden RP, Barabasz AF, Partridge JM, Barta TE, Dubois LG, Huang KH, Mabbett SR, Silinski MA, Steed PM, Hall SE. 2008. Small molecule inhibitors of Hsp90 potently affect inflammatory disease pathways and exhibit activity in models of rheumatoid arthritis. *Arthritis Rheum* 58:3765–3775.
- Sharp FR, Massa SM, Swanson RA. 1999. Heat-shock protein protection. *Trends Neurosci* 22:97–99.
- Soga S, Akinaga S, Shiotsu Y. 2013. Hsp90 inhibitors as anti-cancer agents, from basic discoveries to clinical development. *Curr Pharm Des* 19:366–376.
- Sonoda H, Prachasilchai W, Kondo H, Yokota-Ikeda N, Oshikawa S, Ito K, Ikeda M. 2010. The protective effect of radicicol against renal ischemia-reperfusion injury in mice. *J Pharmacol Sci* 112:242–246.
- Stetler RA, Gan Y, Zhang W, Liou AK, Gao Y, Cao G, Chen J. 2010. Heat shock proteins: Cellular and molecular mechanisms in the central nervous system. *Prog Neurobiol* 92:184–211.
- Sun Y, Ouyang YB, Xu L, Chow AM, Anderson R, Hecker JG, Giffard RG. 2006. The carboxyl-terminal domain of inducible Hsp70 protects from ischemic injury in vivo and in vitro. *J Cereb Blood Flow Metab* 26:937–950.
- Supko JG, Hickman RL, Grever MR, Malspeis L. 1995. Preclinical pharmacologic evaluation of 2geldanamycin as an antitumor agent. *Cancer Chemother Pharmacol* 36:305–315.
- Tsan MF, Gao B. 2009. Heat shock proteins and immune system. *J Leukoc Biol* 85:905–910.
- Webster CM, Hokari M, McManus A, Tang XN, Ma H, Kacimi R, Yenari MA. 2013. Microglial P2Y12 deficiency/inhibition protects against brain ischemia. *PLoS One* 8:e70927.
- Xiao N, Callaway CW, Lipinski CA, Hicks SD, DeFranco DB. 1999. Geldanamycin provides posttreatment protection against glutamate-induced oxidative toxicity in a mouse hippocampal cell line. *J Neurochem* 72:95–101.
- Xu L, Ouyang YB, Giffard RG. 2003. Geldanamycin reduces necrotic and apoptotic injury due to oxygen-glucose deprivation in astrocytes. *Neurol Res* 25:697–700.
- Yenari MA, Liu J, Zheng Z, Vexler ZS, Lee JE, Giffard RG. 2005. Antiapoptotic and anti-inflammatory mechanisms of heat-shock protein protection. *Ann N Y Acad Sci* 1053:74–83.
- Yenari MA, Xu L, Tang XN, Qiao Y, Giffard RG. 2006. Microglia potentiate damage to blood-brain barrier constituents: Improvement by minocycline in vivo and in vitro. *Stroke* 37:1087–1093.
- Zheng Z, Kim JY, Ma H, Lee JE, Yenari MA. 2008. Anti-inflammatory effects of the 70 kDa heat shock protein in experimental stroke. *J Cereb Blood Flow Metab* 28:53–63.